MSDE

PAPER

View Article Online
View Journal

Cite this: DOI: 10.1039/d0me00016g

Influence of immobilized cations on the thermodynamic signature of hydrophobic interactions at chemically heterogeneous surfaces†

Hongseung Yeon,[a] Chenxuan Wang,[b] Samuel H. Gellman *[b] and Nicholas L. Abbott *[c]

Hydrophobic interactions play a central role in bioinspired strategies for molecular self-assembly in water, yet how these interactions are encoded by chemically heterogeneous interfaces is poorly understood. We report an experimental investigation of the influence of immobilized polar groups (amine) and cations (ammonium and guanidinium) on enthalpic and entropic contributions to hydrophobic interactions mediated by methyl-terminated surfaces at temperatures ranging from 298 K to 328 K and pH values between 3.5 to 10.5. We use our measurements to calculate the change in free energy (and enthalpic and entropic components) that accompanies transfer of each surface from aqueous TEA containing 60 vol% methanol into aqueous TEA (*i.e.*, transfer free energy that characterizes hydrophobicity). We find the thermodynamic signature of the pure methyl surface (positive transfer enthalpy and entropy) to be altered qualitatively by incorporation of amine or guanidinium groups into the surface (negative transfer enthalpy and near zero transfer entropy). In contrast, ammonium groups immobilized on a methyl surface do not change the thermodynamic signature of the hydrophobic interaction. Compensation of entropy and enthalpy is clearly evident in our results, but the overall trends in the transfer free energies are dominated by enthalpic effects. This observation and others lead us to hypothesize that the dominant effect of the immobilized charged or polar groups in our experiments is to influence the number or strength of hydrogen bonds formed by interfacial water molecules adjacent to the nonpolar domains. Overall, these results provide insight into entropy–enthalpy compensation at chemically heterogeneous surfaces, and generate hypotheses and a rich experimental dataset for further exploration *via* simulation.

Received 1st February 2020,
Accepted 12th March 2020

DOI: 10.1039/d0me00016g

rsc.li/molecular-engineering

Design, System, Application

This paper advances our understanding of molecular design rules for hydrophobically-driven interactions between molecules and surfaces. While hydrophobic interactions are widely used to assemble soft material systems (comprised of synthetic and biological molecules), we do not yet understand design rules for hydrophobic interactions in chemically heterogeneous systems. Elucidation of these rules will enable rational design of complex supramolecular structures and tribological properties of surfaces in aqueous systems, and provide insights into the properties and functions of biological assemblies (*e.g.*, cell membranes).

Introduction

The term "hydrophobic interaction" refers to the tendency of nonpolar molecules or surfaces to self-associate in aqueous environments. These water-mediated interactions contribute to processes that underlie formation of remarkably complex supramolecular structures in biological systems such as association of proteins into functional complexes and self-assembly of

[a] *Department of Chemical and Biological Engineering, University of Wisconsin-Madison, 1415 Engineering Drive, Madison, Wisconsin 53706, USA*
[b] *Department of Chemistry, University of Wisconsin-Madison, 1101 University Avenue, Madison, Wisconsin 53706, USA. E-mail: gellman@chem.wisc.edu*
[c] *Smith School of Chemical and Biomolecular Engineering, Cornell University, Ithaca, New York 14853, USA. E-mail: nla34@cornell.edu*

† Electronic supplementary information (ESI) available: Fig. S1: representative force histograms of adhesive forces measure between nonpolar SAMs. Fig. S2: characterization of the atomic composition of pure- and mixed-component amine or guanidine SAMs. Fig. S3: calibration of the spring constant of AFM cantilevers. Fig. S4: temperature reversibility of mean adhesive forces. Fig. S5: pH dependence of mean adhesive forces. Fig. S6: imaginary processes used to evaluate the transfer free energy. Fig. S7: comparison of experimentally-determined and calculated transfer free energies. Fig. S8: comparison of experimentally-determined and atomic-composition-weighted transfer free energies. Table S1: statistical information of the force measurements. Table S2: four possible scenarios in terms of the association/dissociation of counter ions with the protonated amine groups. See DOI: 10.1039/d0me00016g

cell membranes, and formation of RNA tertiary structures.[1–8] The hydrophobic interaction is primarily a consequence of the dynamic structuring of water at nonpolar interfaces.[4] Molecular dynamics (MD) simulations have predicted the size of nonpolar solutes and temperature to influence the thermodynamics of hydrophobic interactions.[4,9–13] At ambient temperature, the hydration of small nonpolar solutes (radius of curvature <1 nm) leads to an enhancement of hydrogen bonding between water molecules relative to bulk water, resulting in a decrease in orientational entropy. To minimize this entropic penalty, small nonpolar solutes tend to self-associate in water.[4,9] In contrast, for large nonpolar solutes (radius of curvature >1 nm) or macroscopic surfaces, a low interfacial curvature inhibits formation of a network of hydrogen bonds characteristic of bulk water. This geometric frustration leads to an increase in orientational entropy but unfavorable enthalpic interactions.[4,13] Accordingly, the tendency of large non-polar solutes or macroscopic surfaces to self-associate in water is largely driven by enthalpy.[4,9–13]

Although many studies have explored the thermodynamics of hydrophobic interactions using homogeneous nonpolar solutes, the degree to which chemical heterogeneity changes the way in which enthalpy and entropy compensate each other to drive hydrophobic interactions has not been fully elucidated.[4,7,9–11] In this paper, we move to investigate the influence of polar groups and cations immobilized at nonpolar surfaces on the thermodynamic signatures of hydrophobic interactions mediated by those surfaces. The work is motivated by our recent experimental observation that immobilized charged or polar groups can modulate the strength of hydrophobic adhesion mediated by adjacent nonpolar domains.[14,15] These conclusions were supported by measurements performed using two independent model systems, sequence-specific oligopeptides and mixed self-assembled monolayers (SAMs).[14,15] In particular, we demonstrated that protonation of amine groups within mixed amine/methyl-terminated SAMs enhances the strength of hydrophobic adhesion, whereas replacement of ammonium with guanidinium cations leads to a weakening of the strength of the hydrophobic adhesion.[14] These results generate two important questions: i) why do hydrophobic interactions of mixed amine/methyl surfaces increase in strength upon protonation of the amine groups? And ii) why are mixed guanidinium/methyl surfaces less hydrophobic than mixed ammonium/methyl surfaces? A key goal of this paper is to address these two questions, with a particular focus on elucidating the enthalpic and entropic contributions to the hydrophobic interactions mediated by these chemically heterogeneous surfaces.

To advance our understanding of the thermodynamic origin of the divergent effects of immobilized amine and guanidine groups on hydrophobic interactions, we used atomic force microscopy (AFM) to perform temperature-dependent force measurements with mixed monolayers formed from 40% 11-aminoundecanethiol or 40% 11-guanidinoundecanethiol and 60% 1-decanethiol on gold films. For comparison, we also prepared pure monolayers terminated with methyl (100% 1-decanethiol), amine (100% 11-aminoundecanethiol), or guanidine (100% 11-guanidinoundecanethiol) groups. We measured the pull-off forces between the mixed monolayer surfaces and a methyl-terminated AFM tip at temperatures between 298 K and 328 K and pH values ranging from 3.5 to 10.5. Using a previously reported methodology,[14] we quantified adhesive forces arising from hydrophobic interactions by adding 60 vol% methanol into aqueous triethanolamine (TEA, 10 mM). In this paper, we interpret the force measurements using Johnson–Kendall–Roberts (JKR) theory[16] to evaluate the free energy change (per unit area) accompanying the transfer of each mixed monolayer surface from aqueous TEA containing 60 vol% methanol into aqueous TEA (*i.e.*, a free energy per unit area that characterizes hydrophobicity of the surface). The temperature-dependence of this transfer free energy was analyzed to identify enthalpic (*i.e.*, transfer enthalpy) and entropic (*i.e.*, transfer entropy) contributions. Past studies have used temperature-dependent force measurements to quantify the strength of hydrophobic interactions mediated by nonpolar monolayers[17] or polymers.[18] The results reported in this paper go beyond these prior studies by focusing on the effects of specific immobilized polar groups and cations on hydrophobic interactions.

Method and materials

Materials

1-Decanethiol ($C_{10}H_{21}SH$, 96%), 1-dodecanethiol ($C_{12}H_{25}SH$, 98%), triethanolamine HCl (TEA, 99%), methanol (anhydrous, 99.8%), and ethanol (reagent, anhydrous, denatured) were purchased from Sigma-Aldrich (Milwaukee, WI). 11-Aminoundecanethiol ($AmC_{11}H_{22}SH$) and 11-guanidinoundecanethiol ($GdmC_{11}H_{22}SH$) were purchased from Prochimia (Poland). Ethanol (anhydrous, 200 proof) for rinsing was purchased from Decon Labs (King of Prussia, PA). The resistivity of de-ionized water used in this study was 18.2 MΩ cm. All chemicals were used as received without further purification. The AFM tips were purchased from Bruker Nano Company (Santa Barbara, CA). Silicon wafers were purchased from Silicon Sense (Nashua, NH).

Preparation of chemically functionalized AFM tips

Triangular-shaped cantilevers with nominal spring constant of 0.1 N m^{-1} were used for all force measurements. AFM tips were coated sequentially with a 2 nm layer of titanium and a 20 nm layer of gold by physical vapor deposition using an electron beam evaporator (Tek-Vac Industries, Brentwood, NY). The rates of deposition of titanium and gold were controlled at ~0.2 Å s^{-1}. The pressure and temperature in the evaporator was maintained under 1.2×10^{-6} Torr and 333 K throughout evaporation processes to obtain high quality of samples. Following deposition of the gold, the AFM tips were immersed into 1 mM 1-dodecanethiol dissolved in ethanol and incubated overnight. Upon removal from solution, the chemically-modified AFM tips were thoroughly rinsed with

ethanol, dried under a gentle stream of nitrogen and used immediately in the AFM force measurements.

Preparation of pure- or mixed-component SAMs

Silicon wafers were coated sequentially with a 2 nm-thick layer of titanium and a 20 nm-thick layer of gold by physical vapor deposition as described above. For preparation of pure-component SAMs, small pieces of gold-coated silicon wafers (1 cm by 1 cm) were immersed into ethanolic solutions containing 1 mM of the appropriate thiol components (1-decanethiol, 11-aminoundecanethiol, or 11-guadinoundecanethiol) and incubated overnight. The mixed-component SAMs were prepared *via* co-adsorption of 0.4 mM of ω-functionalized undecanethiol ($AmC_{11}H_{22}SH$ or $GdmC_{11}H_{22}SH$) and 0.6 mM of 1-decanethiol ($C_{10}H_{21}SH$) for 3 hours. Upon removal from solution, the chemically modified substrates were alternatively rinsed with ethanol and de-ionized water for 20 seconds, dried with a stream of nitrogen and used immediately in AFM force measurements.

Characterization of pure- or mixed-component SAMs

We prepared five pure- or mixed-component SAMs, as shown in Fig. 1A–E. The pure-component SAMs included i) pure methyl monolayers ("C_{10}") formed from 1-decanethiol, ii) pure amine monolayers ("100% Am") formed from 11-aminoundecanethiol, and iii) pure guanidine monolayers ("100% Gdm") formed from 11-guanidinoundecanethiol. Mixed-component SAMs include i) mixed amine/methyl monolayers ("40% Am") formed from a mixture of 40% 11-aminoundecanethiol and 60% 1-decanethiol and ii) mixed guanidine/methyl monolayers ("40% Gdm") formed from a mixture of 40% 11-guanidinoundecanethiol and 60% 1-decanethiol (in mole fraction).

As detailed previously,[14] we used X-ray photoelectron spectroscopy (XPS) (Thermo Scientific, MA) to confirm the atomic composition of amine and guanidine groups in the mixed-component SAMs to be 37 ± 6% and 38 ± 2%, respectively (Fig. S1†). We also confirmed the optical thicknesses of the monolayers formed on gold surfaces by performing ellipsometry (Gaertner Scientific Corporation, IL) at 632.8 nm with an incident angle of 70° (Fig. 1F). We measured the optical thicknesses of the monolayers formed from 1-dodecanethiol (17.7 ± 0.8 Å, "C_{12}") and 1-decanethiol (12.5 ± 0.8 Å, "C_{10}") to be close to previously reported values.[14,19,22] The optical thicknesses of pure amine monolayers (17.0 ± 0.8 Å, "100% Am") and pure guanidine monolayers (16.8 ± 0.8 Å, "100% Gdm") were observed to be close to that of pure methyl monolayers formed from 1-dodecanethiol, suggesting that the identity of the ω-terminal group does not impact measurably the packing of the monolayers. Additionally, the optical thicknesses of mixed amine/methyl monolayers (15.2 ± 1.0 Å, "40% Am") and mixed guanidine/methyl monolayers (14.6 ± 0.8 Å, "40% Gdm") were intermediate between pure amine or pure guanidine monolayers and 1-decanethiol monolayers, consistent with the atomic composition measured by XPS.

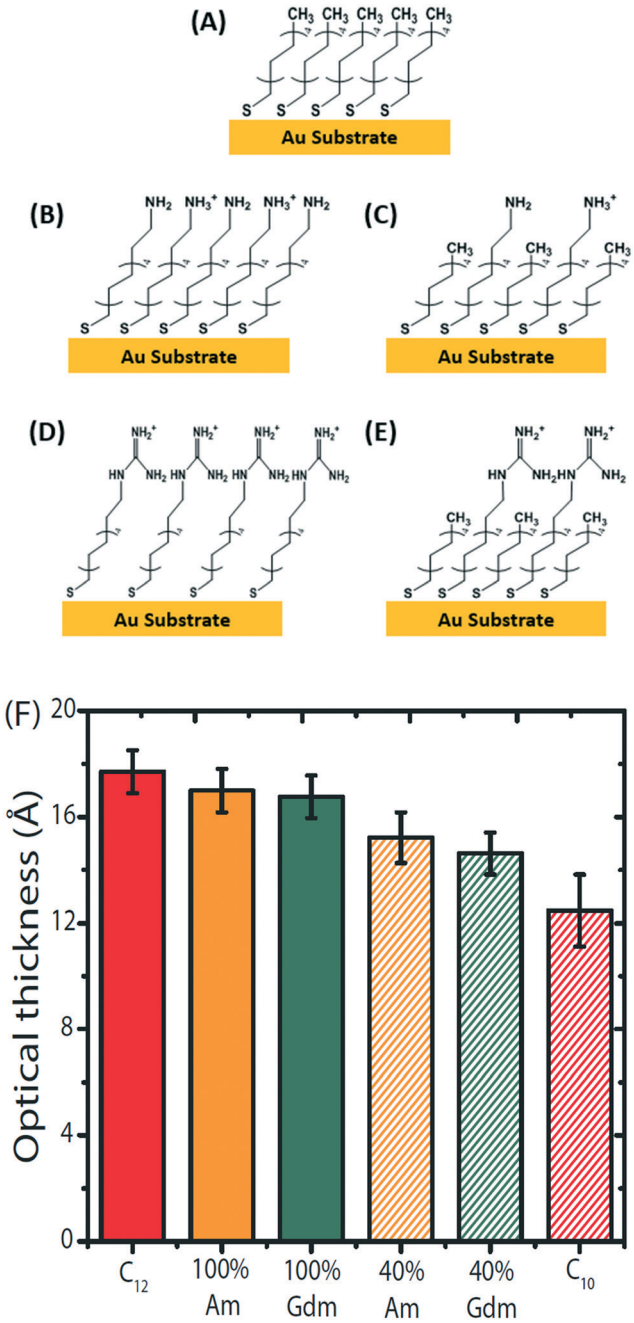

Fig. 1 Pure- and mixed-component self-assembled monolayers (SAMs) presenting methyl (A), amine (B and C), and guanidine (D and E) functional groups at surfaces. The atomic composition of cationic groups in mixed-component SAMs is approximately 40%, as confirmed by XPS. (F) Optical thickness of methyl (1-dodecanethiol ("C_{12}") and 1-decanethiol ("C_{10}")), pure- and mixed-component amine ("100% Am" and "40% Am"), and pure- and mixed-component guanidine ("100% Gdm" and "40% Gdm") SAMs formed on gold-coated substrates. The lateral distribution of the two components within the mixed monolayer is expected to be statistical.

Temperature-dependent AFM force measurements

AFM force measurements were performed using a Nanoscope IIIa Multimode AFM equipped with a fluid cell (Veeco

Metrology Group, Santa Barbara, CA) and temperature-controlled stage (Veeco Metrology Group, Santa Barbara, CA; precision of ±0.5 K). Silicon nitride cantilevers with a nominal spring constant of 0.1 N m^{-1} were used and modified as described above. The spring constants of the cantilevers were calibrated using Sader's method on a PCM-90 Spring Constant Calibration Module (Novascan Technologies, Ames, IA) and determined to be 0.3395 ± 0.007 N m^{-1} (Fig. S2†).[14,19] The influence of temperature on the spring constant of the cantilevers is minor for temperatures ranging from 298 K to 338 K.[20]

We measured pull-off forces required to detach methyl-terminated AFM tips from adhesive contact with the monolayer surfaces used in our study. Over a thousand tip-sample contacts were used to characterize the pull-off forces at temperatures ranging from 298 K to 328 K (steps of 10 K). At each temperature, the samples were thermally equilibrated for 10 minutes prior to performing force measurements. Force curves were recorded with a constant contact time of 500 μs and speeds of 1000 nm s^{-1} for both the approach and retraction of the tip to/from the substrate. At a given temperature, adhesion forces were measured at least 200 times using at least five independently prepared samples (Table S1†). Force distributions were fitted to a Gaussian curve using Origin software (OriginLab Corporation, Northampton, MA) to determine the mean adhesive force (Fig. S3†). Additionally, guided by our past study,[19] we excluded any datasets with non-Gaussian force distributions (*i.e.*, which can arise due to factors such as deformation of the gold-coated tip or attachment of a dust particle to the AFM tip) from our analysis. Error bars presented in the Results section show the standard errors of mean adhesive forces measured using multiple AFM tips, and thus incorporate the error associated with uncertainty in the local AFM tip geometry.

Force measurements were performed in aqueous TEA or 60 vol% methanol added to aqueous TEA in the temperature ranging from 298 K to 328 K. We previously reported that addition of methanol into an aqueous solution can largely eliminate hydrophobic interactions without substantially changing electrical double layer (EDL) interactions mediated by charged groups.[14] Van der Waals interactions in water and water/methanol mixtures are also similar due to similar refractive indices of the two liquids.[19] Accordingly, the difference in adhesive forces measured before and after addition of 60 vol% methanol into aqueous TEA corresponds to the adhesive force arising from hydrophobic interaction.

To change the charge status of surface-immobilized amine and guanidine groups, we adjusted the pH of aqueous TEA to 3.5, 7.0 or 10.5 by using 0.1 M hydrochloric acid (HCl) or 0.1 M sodium hydroxide (NaOH). Dissolved gases were removed using a vacuum pump at 1.0 × 10^{-4} torr for 1 hour prior to performing force measurement (Welch Vacuum-Gardner Denver, Mt. Prospect, IL). The boiling point of 60 vol% methanol added to water is 347 K,[21] approximately 19 K higher than the maximum temperature used in our force measurements (328 K). We measured the effects of temperature on adhesive forces for temperatures ranging from 298 K to 328 K to be reversible (Fig. S4†), to confirm that i) there is no measurable change in composition of 60 vol% methanol added to aqueous TEA due to evaporation during the force measurements and ii) the SAMs are thermally stable over this temperature interval.

Results

Hydrophobic interactions at mixed amine/methyl surfaces

The first measurements reported in this paper were performed to address two questions related to mixed amine/methyl surfaces: (i) how does the incorporation of amine groups into a methyl surface change the thermodynamic signature of a hydrophobic interaction? And (ii) how does protonation of amine groups within mixed amine/methyl surfaces influence the relative contributions of enthalpy and entropy to hydrophobic interactions? The data needed to address these questions are presented in Fig. 2 to 4.

Fig. 2A–C show mean adhesive forces measured between either pure amine surfaces (orange) or mixed amine/methyl surfaces (navy) and a nonpolar AFM tip in aqueous TEA (filled) or 60 vol% MeOH added to aqueous TEA (open) as a function of temperature (from 298 K to 328 K). To change the charge status of the amine groups, we adjusted the pH of the aqueous TEA from 3.5 (A) to 7.0 (B) to 10.5 (C). The choice of pH was guided by a past study that reported surface-immobilized amine groups to be substantially deprotonated at pH 10.5, and largely protonated at pH 7.0.[14] Consistent with this past study, a comparison of Fig. 2A and B reveals that a change in pH from 7.0 to 3.5 does not affect the magnitude of adhesive forces (*i.e.*, amine groups in pure- and mixed-component monolayers are largely protonated at pH ≤ 7.0 (see ESI† Fig. S5 for details)). In contrast, inspection of Fig. 2B and C confirms that the hydrophobic force measured between mixed amine/methyl surfaces and the nonpolar AFM tips increases in magnitude upon lowering the pH from 10.5 to 7.0 (see Introduction and Methods for a description of the methodology used to identify the hydrophobic force).[14] Fig. 2D shows the temperature-dependence of the hydrophobic adhesive force mediated by the mixed amine/methyl surfaces at various pHs. The magnitude of the hydrophobic force decreases with increasing temperature from 298 K to 328 K (*e.g.*, the force decreases from 5.4 ± 0.7 nN to 2.8 ± 0.5 nN at pH 7.0 and from 3.2 ± 0.8 nN to 1.6 ± 0.7 nN at pH 10.5). For comparison, Fig. 3 shows adhesion force measurements performed with pure methyl surfaces, with magnitudes independent of pH. The statistical significance of these trends is discussed below.

We analyzed the adhesion force measurements described above using JKR theory[16] to evaluate the work of adhesion (*i.e.*, the free energy change arising from adhesive interactions) between two contacting surfaces. Fig. 3A provides a schematic illustration of an adhesive interaction between a methyl-terminated SAM (s1) formed on an AFM tip and a second (*e.g.*, pure methyl or mixed amine/methyl) SAM (s2) formed on a substrate in the presence of either aqueous TEA ("Aqueous TEA") or 60 vol% MeOH added to aqueous TEA

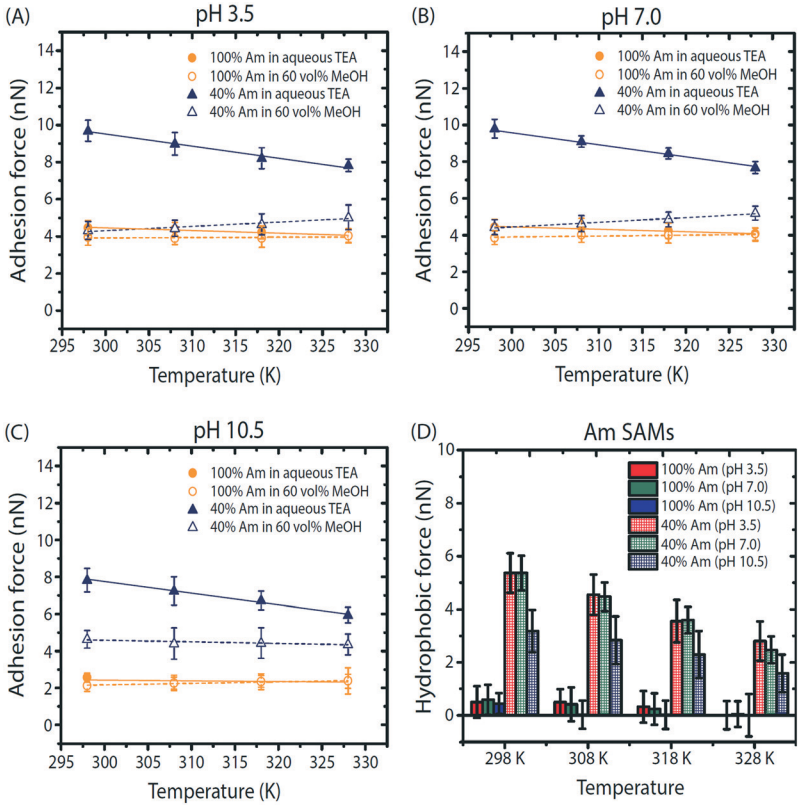

Fig. 2 (A–C) Mean adhesive forces measured between pure amine (or ammonium) surfaces ("100% Am", orange circle) or mixed amine/methyl (or ammonium/methyl) surfaces ("40% Am", navy triangle) and a methyl-terminated AFM tip as a function of temperature from 298 K to 328 K in either aqueous TEA (filled) or 60 vol% MeOH added to aqueous TEA ("60 vol% MeOH"; open) at pH 3.5 (A), 7.0 (B) and 10.5 (C), respectively. (D) Mean adhesive forces arising from hydrophobic interactions between pure amine (or ammonium) surfaces (solid) or mixed amine/methyl (or ammonium/methyl) surfaces (grid) and the nonpolar AFM tips as a function of temperature from 298 K to 328 K measured at pH 3.5 (red), 7.0 (green) or 10.5 (blue), respectively.

("60% MeOH"). Inspection of Fig. 3A reveals that the hydrophobic contribution to the work of adhesion between the SAMs can be evaluated as the sum of the free energy change upon transfer of each of the SAMs from aqueous TEA containing 60 vol% MeOH into aqueous TEA, namely

$$\Delta G_{\mathrm{tr,total}}(60\%\ \mathrm{MeOH} \rightarrow \mathrm{TEA}) = \Delta G_{\mathrm{tr,s1}}(60\%\ \mathrm{MeOH} \rightarrow \mathrm{TEA}) + \Delta G_{\mathrm{tr,s2}}(60\%\ \mathrm{MeOH} \rightarrow \mathrm{TEA}) \quad (1)$$

The transfer free energy (per unit area) of the methyl-terminated SAM ($\Delta G_{\mathrm{tr,CH_3}}(60\%\ \mathrm{MeOH} \rightarrow \mathrm{TEA})$ where s1 = CH_3) can be evaluated from the force measurements between a pair of methyl-terminated SAMs *via* eqn (S9a) and (S9b) (see section S1†) as

$$\Delta G_{\mathrm{tr,CH_3}}(60\%\ \mathrm{MeOH} \rightarrow \mathrm{TEA}) = \frac{1}{3\pi R}\left(F_{\mathrm{ad,CH_3\text{–}CH_3,TEA}} - F_{\mathrm{ad,CH_3\text{–}CH_3,60\%MeOH}}\right) \quad (2)$$

where $F_{\mathrm{ad,CH_3\text{–}CH_3,TEA}}$ and $F_{\mathrm{ad,CH_3\text{–}CH_3,60\%MeOH}}$ are the adhesive forces measured between two methyl-terminated SAMs in aqueous TEA or 60 vol% MeOH added to aqueous TEA, respectively. R is the effective radius of the AFM tip (R_1 = 53 ± 5 nm)[14] and monolayer surfaces ($R_2 = \infty$) (where $R^{-1} = R_1^{-1} + R_2^{-1}$). The transfer free energy (per unit area) of the second (functionalized) SAM ($\Delta G_{\mathrm{tr,func}}$ (60% MeOH → TEA) where s2 = func) can be evaluated *via* eqn (S18)† as

$$\Delta G_{\mathrm{tr,func}}(60\%\ \mathrm{MeOH} \rightarrow \mathrm{TEA}) = \frac{2}{3\pi R}\left(F_{\mathrm{ad,CH_3\text{-}func,TEA}} - F_{\mathrm{ad,CH_3\text{-}func,60\%MeOH}}\right) - \frac{1}{3\pi R}\left(F_{\mathrm{ad,CH_3\text{–}CH_3,TEA}} - F_{\mathrm{ad,CH_3\text{–}CH_3,60\%MeOH}}\right) \quad (3)$$

where $F_{\mathrm{ad,CH_3\text{-}func,TEA}}$ and $F_{\mathrm{ad,CH_3\text{-}func,60\%MeOH}}$ are the adhesive forces measured between the methyl-terminated AFM tip and functionalized SAM in either aqueous TEA or 60 vol% MeOH added to aqueous TEA, respectively.

We evaluated the entropic contribution to the transfer free energy (*i.e.*, entropy change upon transfer from 60% MeOH to aqueous TEA) for methyl-terminated SAMs ($\Delta S_{\mathrm{tr,CH_3}}$) and functionalized SAMs ($\Delta S_{\mathrm{tr,func}}$) by taking the derivative of the transfer free energy with respect to temperature at constant pressure (p):

$$\Delta S_{\mathrm{tr,CH_3}} = -\left(\frac{\partial \Delta G_{\mathrm{tr,CH_3}}}{\partial T}\right)_p = -\frac{1}{3\pi R}\left(\frac{\partial\left(F_{\mathrm{ad,CH_3\text{–}CH_3,TEA}} - F_{\mathrm{ad,CH_3\text{–}CH_3,60\%MeOH}}\right)}{\partial T}\right)_p \quad (4a)$$

$$\Delta S_{\mathrm{tr,func}} = -\left(\frac{\partial \Delta G_{\mathrm{tr,func}}}{\partial T}\right)_p = -\frac{1}{3\pi R}\frac{\partial}{\partial T}\left[2\left(F_{\mathrm{ad,CH_3\text{-}func,TEA}} - F_{\mathrm{ad,CH_3\text{-}func,60\%MeOH}}\right) - \left(F_{\mathrm{ad,CH_3\text{–}CH_3,TEA}} - F_{\mathrm{ad,CH_3\text{–}CH_3,60\%MeOH}}\right)\right]_p \quad (4B)$$

We then calculated the enthalpic contribution to the transfer free energy (*i.e.*, enthalpy change upon transfer from 60% MeOH to aqueous TEA) for methyl-terminated SAMs ($\Delta H_{\mathrm{tr,CH_3}}$) and functionalized SAMs ($\Delta H_{\mathrm{tr,func}}$) by incorporating eqn (4a) and (4b) into eqn (2) and (3), respectively.

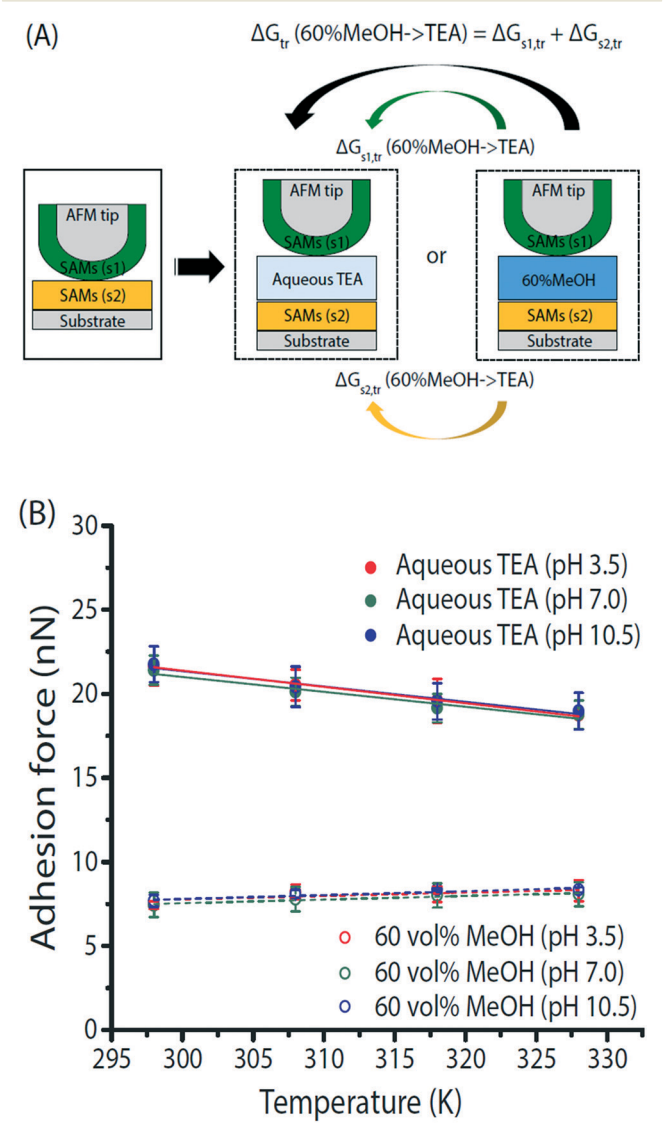

Fig. 3 (A) Schematic illustration of adhesion between the SAMs (s1 and s2) formed on an AFM tip and a substrate in the presence of aqueous TEA ("Aqueous TEA" in light blue) or 60 vol% MeOH added to aqueous TEA ("60% MeOH" in dark blue). The free energy change upon transfer of the two SAMs from aqueous TEA containing 60 vol% MeOH into aqueous TEA corresponds to hydrophobic contribution to the adhesive interactions between the SAMs (*i.e.*, total transfer free energy, $\Delta G_{\mathrm{tr,total}}$ (60% MeOH → TEA). (B) Mean adhesive forces between methyl-terminated SAMs formed from 1-dodecanethiol (on AFM tip) and 1-decanethiol (on substrate) as a function of temperature from 298 K to 328 K measured in aqueous TEA (filled circle, solid lines) or 60 vol% MeOH added to aqueous TEA (open circle, dashed lines) at pH 3.5 (red), 7.0 (green), or 10.5 (blue), respectively.

To assess the statistical significance of the transfer free energy calculated as a function of pH and temperature (*i.e.*, single observation) from eqn (2) and (3), we randomly selected 25 observations at each pH and temperature. Using the 25 observations, we calculated a mean transfer free energy. This selection procedure was repeated 100 times (*i.e.*, 2500 random selections in total with replacement (*i.e.*, data selected from the observation set were returned to the pool of measured values for further possible selection) at each pH and temperature). The transfer free energies plotted in Fig. 4A were estimated with this procedure, and used to calculate the transfer entropies and enthalpies. For example, the transfer free energies of pure methyl surfaces at pH 7.0 are shown in Fig. 4A (using data shown in Fig. 3B). Measurements at pH 3.5 and 10.5 were indistinguishable from pH 7.0 (see Fig. 3). We calculated the transfer entropy of the pure methyl surfaces *via* eqn (4) by applying a linear regression to the plot of transfer free energy *versus* temperature shown in Fig. 4A (the transfer entropy is not measurably different for temperatures ranging from 298 K to 328 K). This procedure revealed the transfer entropy of the pure methyl surface to be 0.25 ± 0.04 mJ m^{-2} K^{-1}. The corresponding transfer enthalpy was also determined to be positive (endothermic; 105 ± 6 mJ m^{-2}). Overall, these results are consistent with prior estimates of these quantities for planar non-polar surfaces.[4,9–13]

We performed multiple *t*-tests to assess the statistical significance of differences in transfer entropies and the transfer enthalpies reported in this paper. The absence of a statistical difference at a significance level of 99% was marked in a single asterisk (*). The double asterisk (**) indicates the presence of statistical difference at a significance level of 99%. Below we use the experimentally determined transfer free energies, entropies and enthalpies to advance our understanding of the impact of immobilized amine or ammonium groups on hydrophobic interactions.

How does the thermodynamic signature of a hydrophobic interaction change upon incorporation of amine groups into a methyl surface? We addressed this question as context for understanding how protonation of amine groups in mixed amine/methyl surfaces impacts the thermodynamic signature of hydrophobic interactions. Fig. 4B and C show the transfer entropy and transfer enthalpy (at 298 K) of mixed amine/methyl surfaces at 10.5 (blue). For comparison, we also show results with pure methyl and pure amine surfaces. Inspection of Fig. 4B and C reveals that, at pH 10.5, where amine groups are largely deprotonated within the mixed amine/methyl

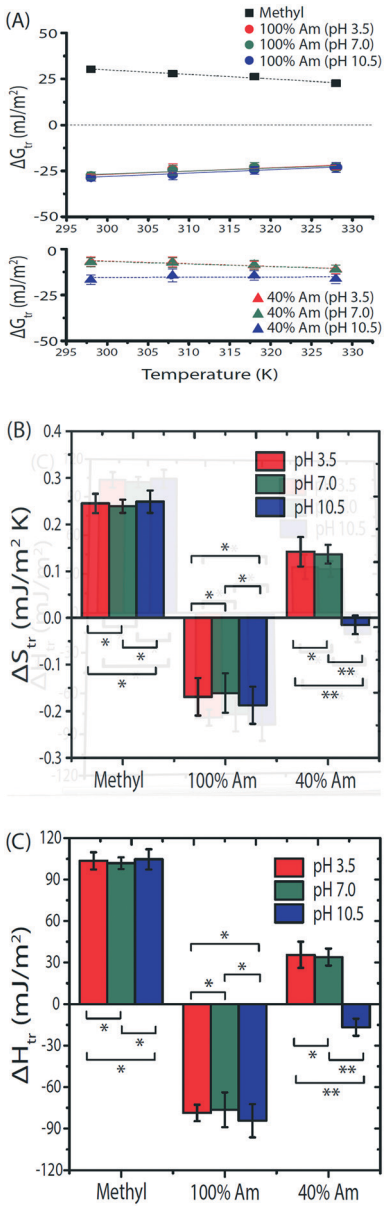

Fig. 4 (A) Transfer free energy (ΔG_{tr}) of pure amine (or ammonium) surfaces ("100% Am", circle) and mixed amine/methyl (or ammonium/methyl) surfaces ("40% Am", triangle) as a function of temperature from 298 K to 328 K measured at pH 3.5 (red), 7.0 (green), or 10.5 (blue), respectively. The transfer free energy is the change in free energy upon transfer of the indicated surface from aqueous TEA containing 60% MeOH to aqueous TEA and thus it corresponds to the free energy change upon "turning on" the hydrophobic effect. The transfer free energy for pure methyl surfaces is plotted in black. (B) Transfer entropy (ΔS_{tr}) of pure amine (or ammonium) surfaces and mixed amine/methyl (or ammonium/methyl) surfaces calculated *via* eqn (2)–(4) from Fig. 4A. (C) Transfer enthalpy (ΔH_{tr}) of pure amine (or ammonium) surfaces and mixed amine/methyl (or ammonium/methyl) surfaces at 298 K calculated *via* eqn (2)–(4) from Fig. 4A and B. In Fig. 4B and C, the absence of statistical difference in transfer entropies and transfer enthalpies is indicated by a single asterisk (*) at a significance level of 99%. The double asterisk (**) indicates the presence of statistical difference in transfer entropies and enthalpies.

surfaces, the transfer enthalpy is favorable (exothermic; −17 ± 6 mJ m^{-2}) and accompanied by a very small transfer entropy (−0.02 ± 0.02 mJ m^{-2} K^{-1}). This result is in striking contrast to a pure methyl surface (also shown in Fig. 4B and C) which, as noted above, is characterized by a transfer enthalpy that is unfavorable (endothermic; 105 ± 6 mJ m^{-2}) and a compensating positive transfer entropy (0.25 ± 0.04 mJ m^{-2} K^{-1}). This comparison reveals that incorporation of amine groups into a methyl surface leads to a qualitative change in the enthalpic and entropic contributions to the transfer free energy underlying the hydrophobic interaction encoded by the surface.

How does the thermodynamic signature of the hydrophobic interaction of a mixed amine/methyl surface change upon protonation of the amine groups? Inspection of Fig. 4A (lower panel) reveals that transfer free energies of mixed amine/methyl surfaces increase with protonation of the amine groups (pH 7.0 differs from pH 10.5). This result indicates that transfer of a mixed amine/methyl surface from aqueous TEA containing 60 vol% MeOH into aqueous TEA is more favorable than the transfer of a mixed ammonium/methyl surface. Furthermore, the charge status of the amine groups impacted the temperature-dependence of the transfer free energies of the mixed amine/methyl surfaces. For instance, the transfer free energies measured at pH 3.5 and 7.0 decreased with increasing temperature, whereas no significant temperature dependence was observed at pH 10.5 (Fig. 4A, lower panel).

Fig. 4B and C show the corresponding transfer entropies and enthalpies at pH 3.5 (red), 7.0 (green) and 10.5 (blue). Inspection of the data reveals that protonation of amine groups within mixed amine/methyl surfaces, achieved by lowering pH from 10.5 to 7.0 or 3.5, causes the transfer enthalpy (at 298 K) to change from −17 ± 6 mJ m^{-2} (exothermic at pH 10.5) to 34 ± 6 mJ m^{-2} (endothermic at pH 3.5 or 7.0) while the transfer entropies increase from −0.02 ± 0.02 mJ m^{-2} K^{-1} (pH 10.5) to 0.14 ± 0.02 mJ m^{-2} K^{-1} (pH 3.5 or 7.0; the transfer entropy and transfer enthalpy at pH 3.5 and 7.0 are not statistically different at a significance level of 99%). Interestingly, after protonation of the amine group, the enthalpic and entropic contributions to the transfer free energy are similar in sign to those of the pure methyl surface. Overall, these data suggest that amine groups within mixed amine/methyl surfaces perturb the thermodynamics of solvation of the interface to an extent that is greater than when ammonium groups are incorporated into the interface. We return to this observation in the Discussion.

We also compared the pH-dependent enthalpic and entropic components of the transfer free energy of the mixed amine/methyl surfaces to a pure amine surface (Fig. 4B and C). Inspection of Fig. 4A (upper panel) reveals that the transfer free energies of pure amine surfaces are favorable and independent of pH for 3.5 to 10.5 (at a significance level of 99%). Although protonation of pure amine surfaces increases the strength of water-mediated adhesion to a pure methyl surface (Fig. 2), the pH-dependence of the adhesive forces are the same in aqueous TEA and 60 vol% MeOH

added to aqueous TEA (also see Fig. 2). In contrast, as described above, the mixed amine/methyl surfaces do show a strong pH-dependent transfer free energy. Overall, this result highlights the non-additivity of water-mediated interactions at chemically heterogeneous surfaces.

Comparison of mixed ammonium/methyl and guanidinium/methyl surfaces

The third key question that we address through the experiments reported in this paper revolves around the relative influence of immobilized ammonium and guanidinium cations on hydrophobic interactions at nonpolar surfaces: what are the differences in enthalpic and entropic contributions to the transfer free energies that underlie the observation that mixed guanidinium/methyl surfaces generate much weaker hydrophobic interactions than mixed ammonium/methyl surfaces? Fig. 5 shows adhesive forces measured between mixed guanidinium/methyl surfaces and nonpolar AFM tips in aqueous TEA or 60 vol% MeOH added to aqueous TEA. In contrast to the mixed ammonium/methyl surfaces (Fig. 2; pH 3.5 or 7.0), upon addition of 60 vol% MeOH, the adhesive forces mediated by the guanidinium/methyl surfaces change very little. Although the forces measured at higher temperatures appear to be slightly larger in 60% MeOH than aqueous TEA (Fig. 5A–C), the differences are not statistically significant. Overall, this result confirms our prior conclusion that immobilized guanidinium cations greatly diminish hydrophobic adhesion mediated by nonpolar domains.[14] In addition, while the differences in the adhesive forces measured in 60% MeOH and aqueous TEA (Fig. 5D) are near zero, we emphasize that the hydrophobic force reflects the transfer free energies of both the methyl-terminated surface on the AFM tip and the mixed guanidinium/methyl surfaces. Thus, the data in Fig. 5 permit identification of statistically significant conclusions regarding the transfer free energy, entropy and enthalpy of the mixed guanidinium/methyl surfaces even though the hydrophobic force changes little with temperature (see below).

Fig. 6A shows the transfer free energies of pure guanidinium surfaces (green) and mixed guanidinium/methyl surfaces (purple), and Fig. 6B and C show the entropic and enthalpic contributions to these transfer free energies. Inspection of Fig. 6B and C reveals that the pH-dependence of the transfer free energy of a guanidinium/methyl monolayer is not statistically significant. This is consistent with the high pK_a value of the guanidinium cation. We make two additional observations using data in Fig. 6B and C. First, we compare the mixed guanidinium/methyl surface to the pure methyl

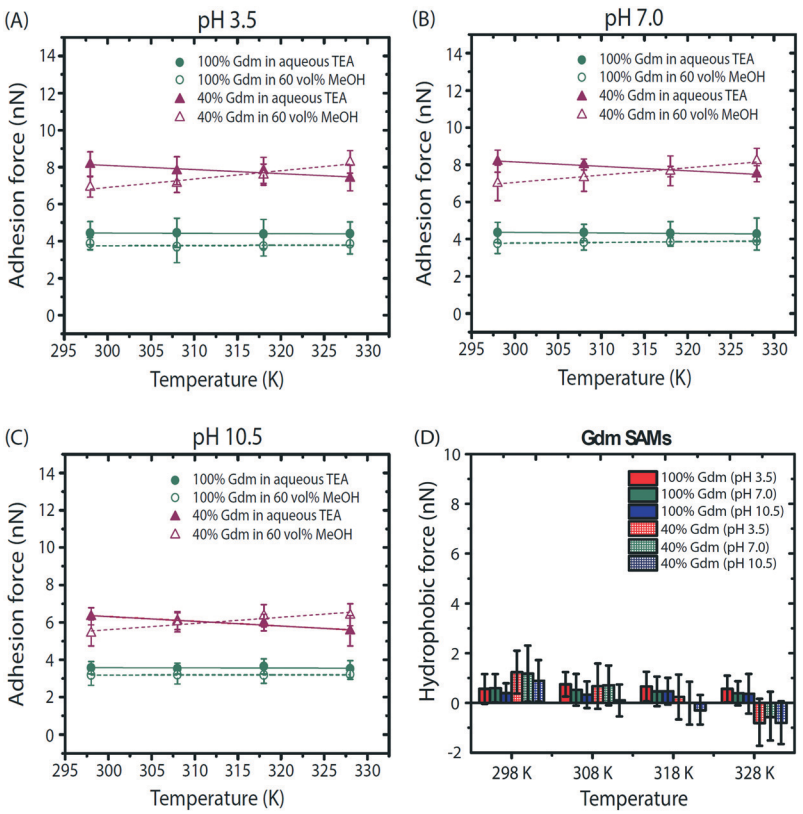

Fig. 5 (A–C) Mean adhesive forces measured between pure guanidinium surfaces ("100% Gdm", green circle) or mixed guanidinium/methyl surfaces ("40% Gdm", purple triangle) and a methyl-terminated AFM tip as a function of temperature from 298 K to 328 K measured in either aqueous TEA (filled) or 60 vol% MeOH added to aqueous TEA ("60 vol% MeOH"; open) at pH 3.5 (A), 7.0 (B) or 10.5 (C), respectively. (D) Mean adhesive forces arising from hydrophobic interactions between pure guanidinium surfaces (solid) or mixed guanidinium/methyl surfaces (grid) and the nonpolar AFM tip as a function of temperature from 298 K to 328 K measured at pH 3.5 (red), 7.0 (green) or 10.5 (blue), respectively.

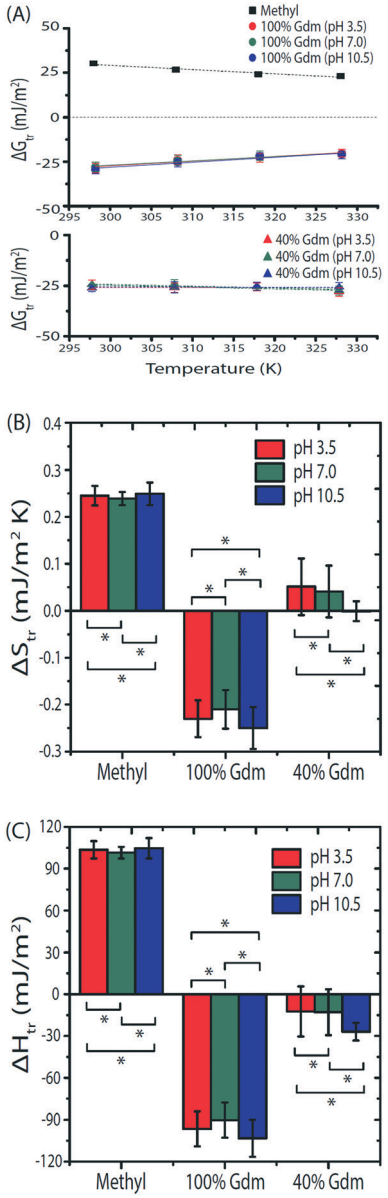

Fig. 6 (A) Transfer free energy (ΔG_{tr}) of pure guanidinium surfaces ("100% Gdm", circle) and mixed guanidinium/methyl surfaces ("40% Gdm", triangle) as a function of temperature from 298 K to 328 K measured at pH 3.5 (red), 7.0 (green), or 10.5 (blue), respectively. The transfer free energy is the change in free energy upon transfer of the indicated surface from aqueous TEA containing 60% MeOH to aqueous TEA and thus it corresponds to the free energy change upon "turning on" the hydrophobic effect. The transfer free energy for pure methyl surfaces is plotted in black. (B) Transfer entropy (ΔS_{tr}) of pure guanidinium surfaces and mixed guanidinium/methyl surfaces calculated *via* eqn (2)–(4) from Fig. 6A. (C) Transfer enthalpy (ΔH_{tr}) of pure guanidinium surfaces and mixed guanidinium/methyl surfaces at 298 K calculated *via* eqn (2)–(4) from Fig. 6A and B. In Fig. 6B and C, the absence of statistical difference in transfer entropies and transfer enthalpies is indicated by a single asterisk (*) at a significance level of 99%. The double asterisk (**) indicates the presence of statistical difference in transfer entropies and enthalpies.

surface. Whereas, as noted above, a pure methyl surface is characterized by an unfavorable enthalpic (endothermic; 105 ± 6 mJ m^{-2}) and favorable entropic (0.25 ± 0.04 mJ m^{-2} K^{-1}) contribution to the transfer free energy, our data reveal that incorporation of guanidinium cations into a methyl surface leads to far smaller transfer entropies (0.05 ± 0.06 mJ m^{-2} K^{-1}) and enthalpies (−12.4 ± 18.0 mJ m^{-2}). More generally, we observe that the transfer free energies of both pure component monolayers (methyl and guanidinium) are characterized by large but compensating transfer enthalpies and entropies. In contrast, the behavior of the mixed guanidinium/methyl surface is strikingly different in that both enthalpic and entropic contributions to the transfer energy are very small and weakly compensating (it is possible that enthalpic and entropic contributions to the transfer free energy are both favorable; the error bars prevent a definitive conclusion).

Next, we compare the thermodynamic signatures of the transfer free energies of the ammonium/methyl (Fig. 4) and guanidinium/methyl surfaces (Fig. 6). We focus the comparison on data obtained at pH 3.5 because the amine group is expected to be fully protonated at pH 3.5. Inspection of these figures reveals that ammonium and guanidinium, when immobilized within a methyl surface, create surfaces with distinct thermodynamic signatures: (i) the transfer entropy for mixed guanidinium/methyl surfaces (0.05 ± 0.06 mJ m^{-2} K^{-1}) is less favorable than for mixed ammonium/methyl surfaces (0.14 ± 0.03 mJ m^{-2} K^{-1}) at pH 3.5 (at a significance level of 99%); and (ii) the transfer enthalpy for mixed guanidinium/methyl surfaces (−12.4 ± 18.0 mJ m^{-2}) is more favorable than for mixed ammonium/methyl surfaces (35.5 ± 9.5 mJ m^{-2}).

We make two additional observations regarding these two classes of surfaces by plotting their transfer free energies along with the enthalpic and entropic components in Fig. 7. First, inspection of Fig. 7 reveals that the extent of compensation of entropic and enthalpic contributions to the transfer free energy is much larger for ammonium/methyl surfaces than guanidinium methyl surfaces. This observation is similar to that made above

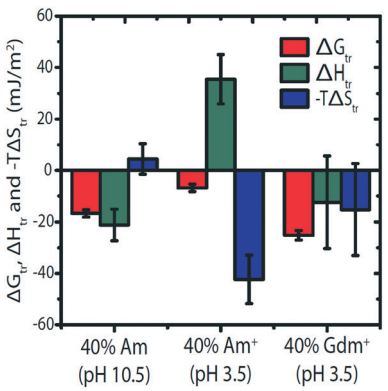

Fig. 7 Transfer free energy (ΔG_{tr}, red), transfer enthalpy (ΔH_{tr}, green), and transfer entropy multiplied by temperature (T) ($-T\Delta S_{tr}$, blue) of mixed amine/methyl surfaces ("40% Am", pH 10.5), mixed ammonium/methyl surfaces ("40% Am^{+}", pH 3.5) and mixed guanidinium/methyl surfaces ("40% Gdm^{+}", pH 3.5) at 298 K. The transfer free energy is the change in free energy upon transfer of the indicated surface from 60% MeOH to aqueous TEA and thus it corresponds to the free energy change upon "turning on" the hydrophobic effect.

in the context of comparing the mixed guanidinium/methyl surface to the pure guanidinium and pure methyl surfaces, and reinforces the conclusion that the mixed guanidinium/methyl surfaces are characterized by small and weakly compensating contributions to the transfer free energy. Second, we observe that the thermodynamic signature of mixed guanidinium/methyl surfaces is closer to that of the mixed amine/methyl surfaces at pH 10.5 (also shown in Fig. 7) than the mixed ammonium/methyl surfaces at pH 3.5. We return to this point below in a discussion of hydrogen bonding between amine, ammonium and guanidinium groups.

Discussion

The results reported in this paper reveal how immobilization of amine, ammonium and guanidinium groups at methyl surfaces can change the thermodynamic signatures of hydrophobic interactions mediated by these surfaces. Whereas a pure methyl surface was found to be characterized by a positive enthalpy and entropy change upon transfer from 60% MeOH to aqueous TEA (*i.e.*, upon "turning on" the hydrophobic effect), the incorporation of amine groups into a methyl surface reversed the thermodynamic signature (negative enthalpy and weakly negative entropy change upon transfer from 60% MeOH to aqueous TEA). The overall decrease in transfer free energy that was measured to accompany incorporation of amine groups into methyl surfaces, which underlies the decrease in strength of hydrophobic adhesion (Fig. 2C and 3B), was dominated by the effect of amine groups on the transfer enthalpy (*i.e.*, enthalpy change upon transfer of the surface from 60% MeOH to aqueous TEA). This presumably reflects, at least in part, the influence of the amine groups on hydrogen bonding between the surface and water (see Table 1).[23–28] The nitrogen atom of the amine is a hydrogen bond acceptor, and computational studies have proposed that this hydrogen bond plays a central role in determining the structure of the first solvation shell of ammonia (see below for additional comments).[27] Computational studies also predict that the structures of the first solvation shells of ammonia and methylamine differ, indicating that caution should be exercised when translating statements about solvation of small molecules in bulk solution to a complex interface of the type used in our experiments.[27] Attempts to evaluate the transfer free energy of the mixed amine/methyl surface from weighted contributions of the transfer free energies of the pure component monolayers were unsuccessful (see ESI† Fig. S7), consistent with non-additivity of interactions at surfaces with nanoscale heterogeneity.

A second key observation reported in this paper is related to the effect of pH on surfaces with mixed amine/methyl groups. Specifically, we measured hydrophobic adhesion and the transfer free energy (*i.e.*, free energy change upon transfer of the surfaces from 60% MeOH to aqueous TEA) to increase with protonation of amine groups in mixed amine/methyl surfaces. We make three comments on this observation. First, although a compensation of entropy and enthalpy accompanies protonation of the amine groups in the mixed amine/methyl surface (Fig. 4B and C), the overall increase in transfer free energy (*i.e.*, hydrophobicity) is dominated by enthalpic effects. Second, and potentially related, after protonation of the amine groups in the mixed amine/methyl surfaces, the thermodynamic signature of the hydrophobic interaction returned to being similar to that of the pure methyl surface. We interpret this result to suggest that the perturbation to the interfacial ordering of water near the mixed amine/methyl surface caused by the presence of the amine groups (and their hydrogen bonding to water) was partially reversed by protonation. When amine and ammonium groups are compared (Table 1),[24] protonation is observed to cause a complex change in the pattern of hydrogen bonding with water. For example, the nitrogen atom of ammonia but not ammonium can serve as a hydrogen bond acceptor to water.[27] Additionally, the N–H of amine is a weaker hydrogen bond donor than the N–H of ammonium (consistent with relative values of N–H···O bond lengths determined from X-ray data and computations).[27] In computational studies, these differences in hydrogen bonding between ammonia and ammonium cause the average number of water molecules (specifically oxygen atoms of the water molecules) located within 3.5 Å of the nitrogen atom to differ (7.2 and 5.4 for ammonia and ammonium, respectively).[27] Protonation of ammonia (to ammonium) also leads to a large increase in hydration free energy (Table 1).[26,27] While our experiments clearly reveal that the thermodynamic signature of the mixed amine/methyl surface moves towards that of a pure methyl surface upon protonation of the amine, molecular simulations and/or spectroscopic measurements are needed to link the measured changes in thermodynamic signature to changes in the charge and hydrogen bonding status of the interface.

The above hypothesis that a change in local solvent structure near amine *versus* ammonium groups (influenced by hydrogen bonding) underlies our experimental observations, while speculative, does receive some general support from a third

Table 1 Comparison of hydration properties of amine, ammonium and guanidinium groups

	Am	Am^+	Gdm^+
Hydration free energy[23–25] (kcal mol^{-1})	−4.3 (ammonia)	−83.0 (ammonium)	−139.0 (guanidinium)
Hydration enthalpy[23–25] (kcal mol^{-1})	−7.9 (ammonia)	−88.0 (ammonium)	−143.9 (guanidinium)
Hydration entropy[23–25] (cal mol^{-1} K^{-1})	−12.1 (ammonia)	−17.8 (ammonium)	−15.2 (guanidinium)
Hydrogen bonding site with water[26] (theoretical)	3 H-bond donor and 1 acceptor sites	4 H-bond donor sites	6 H-bond donor sites
Water coordination numbers (see text for definitions and details)[27,30]	7.2 (ammonia)	5.4 (ammonium)	20.5 (guanidinium)

observation reported in this paper. Specifically, in contrast to the mixed ammonium/methyl surfaces (pH 3.5), we measured mixed guanidinium monolayers to have an exothermic transfer enthalpy, thus causing the latter mixed monolayers to be less hydrophobic (*i.e.*, more favorable free energy change upon transfer of the surface from 60% MeOH to aqueous TEA; Fig. 7). In particular, we observe that the thermodynamic signature of mixed guanidinium/methyl surfaces is most similar to that of the mixed amine/methyl surfaces (at pH 10.5), of the five types of surfaces reported in this paper. Inspection of Table 1 indicates that, when comparing ammonium with guanidinium groups, computations predict that the water coordination number of guanidinium (number of water molecules in the first solvation shell, which for guanidinium extends 5.4 Å from the carbon atom) is greater than that of ammonium (20.5 *versus* 5.4).[27–30] Overall, our results hint that a productive direction of future inquiry may be to explore, using computations, the correlation between the thermodynamic signatures of the surfaces used in our study and the extent to which the surfaces incorporate species (amine, ammonium, guanidinium) that coordinate with water. We emphasize also, however, that an additional key finding reported in this paper is that the properties of the mixed surfaces cannot be anticipated based on measurements of the properties of pure component surfaces. This point is clearly illustrated by the observation that the transfer free energies of the pure methyl and pure amine surfaces do not depend on pH whereas the transfer free energies of the mixed amine/methyl surfaces are strongly dependent on pH (Fig. 3 and 4).

In an effort to provide physical insight into the influence of the charge status of immobilized amine groups on transfer free energies of the mixed amine/methyl surfaces, we compared the transfer free energies measured in this paper to solvation free energies of NH_3/NH_4^+ or $CH_3NH_2/CH_3NH_3^+$ groups dissolved in bulk aqueous/methanolic solutions, respectively (see Fig. S8 and ESI† section S2). Our results reveal that the behaviors of the molecules in bulk solution do not capture how the charge status of amine groups in pure- and mixed-component surfaces changes transfer free energies. The comparison (and lack of agreement between surface and bulk solution transfer free energies) hints that the solvation of functional groups immobilized at surfaces differs from that in bulk solution. For example, the presence of neighboring amine groups may lead to sharing of solvation shells. Additional studies (*e.g.*, molecular dynamics simulations) are needed to understand how the solvation of assemblies of charged, polar and non-polar groups at surfaces differs from that in bulk solution.

Conclusion

The experimental results reported in this paper advance our understanding of the thermodynamics of hydrophobic interactions mediated by chemically heterogeneous surfaces. The key findings are (i) the incorporation of amine groups into methyl surfaces, which weakens hydrophobic interactions, qualitatively changes the thermodynamic signature of the transfer free energy that characterizes the hydrophobic interaction of the mixed amine/methyl surfaces, (ii) protonation of amine groups to ammonium cations within mixed amine/methyl monolayers increases the strength of the hydrophobic interaction and restores the thermodynamic signature (sign of transfer enthalpy and entropy) of the transfer free energy characterizing the hydrophobic interaction of the pure methyl surface, and (iii) in contrast to the mixed ammonium/methyl surfaces, mixed guanidinium/methyl monolayers exhibit an exothermic transfer enthalpy which causes them to be less hydrophobic (*i.e.*, more favorable transfer free energy) and to exhibit a thermodynamic signature closest to the mixed amine/methyl surfaces characterized in this paper (of the five types of surfaces investigated).

From these measurements we make two generalizations that lead to hypotheses for possible future investigation. First, although compensation of entropy and enthalpy is clearly evident in almost all of our results, the overall trends in the transfer free energies characterizing hydrophobic interactions are dominated by enthalpic effects. This observation leads us to hypothesize that an important effect of the immobilized charged or polar groups in our experiments is to influence the number or strength of hydrogen bonds formed between water molecules adjacent to the nonpolar domains of the surfaces. Second, our results hint at a possible correlation between the thermodynamic signatures of the surfaces and the extent to which the surfaces incorporate species that can coordinate with water (strongly water coordinating species reverse the signature of the hydrophobic interaction measured with pure methyl surfaces). This observation also suggests molecular hypotheses that could be explored *via* use of molecular simulations.

Overall, our observations of the influence of immobilized amine and guanidine groups on enthalpy–entropy compensation underlying hydrophobic interactions at nonpolar surfaces highlight the non-additive nature of water-mediated interactions at these surfaces. Specifically, the transfer free energies of mixed monolayer surfaces calculated from JKR theory deviate quantitatively from the transfer free energies of pure component monolayers weighted by their surface composition. These transfer free energies provide an experimental benchmark against which molecular simulations can be compared, thus enabling additional insight into the structure and dynamics of interfacial water at chemically heterogeneous surfaces.

Conflicts of interest

The authors declare no conflicts of interests with the contents of this manuscript.

Acknowledgements

This research was primarily supported by the Army Research Office (W911NF-19-1-0071 W911NF-16-1-0154 W911NF-15-1-0568), with additional partial support from the National Science Foundation (CBET-1803409). Use of the facilities of the Cornell Center for Materials Research is also acknowledged

(NSF Grant DMR-1719875). We thank Dr. Lynn Johnson at the Cornell Statistical Consulting Unit for her contributions to the statistical analyses. Hongseung Yeon acknowledges partial financial support from the Department of Chemical and Biological Engineering at University of Wisconsin-Madison.

References

1 C. Tanford, The hydrophobic effect and the organization of living matter, *Science*, 1978, **200**(4345), 1012–1018.
2 R. F. Tabor, F. Grieser, R. R. Dagastine and D. Y. C. Chan, The hydrophobic force: measurements and methods, *Phys. Chem. Chem. Phys.*, 2014, **16**, 18065–18075.
3 D. Chandler, Hydrophobicity: Two faces of water, *Nature*, 2002, **417**, 491.
4 D. Chandler, Interfaces and the driving force of hydrophobic assembly, *Nature*, 2005, **437**, 640–647.
5 E. E. Meyer, K. J. Rosenberg and J. Israelachvili, Recent progress in understanding hydrophobic interactions, *Proc. Natl. Acad. Sci. U. S. A.*, 2006, **103**(43), 15739–15746.
6 M. E. Paulaitis, S. Garde and H. S. Ashbaugh, The hydrophobic effect, *Curr. Opin. Colloid Interface Sci.*, 1996, **1**, 376–383.
7 N. T. Southall, K. A. Dill and A. D. J. Haymet, A view of the hydrophobic effect, *J. Phys. Chem. B*, 2002, **106**(3), 521–533.
8 D. Lombardo, M. A. Kiselev, S. Magazù and P. Calandra, Amphiphiles self-assembly: Basic concepts and future perspectives of supramolecular approaches, *Adv. Condens. Matter Phys.*, 2015, **151683**, 22.
9 D. M. Huang and D. Chandler, Temperature and length scale dependence of hydrophobic effects and their possible implications for protein folding, *Proc. Natl. Acad. Sci. U. S. A.*, 2000, **97**, 8324–8327.
10 K. Lum, D. Chandler and J. D. Weeks, Hydrophobicity at small and large length scales, *J. Phys. Chem. B*, 1999, **103**, 4570–4577.
11 S. Rajamani, T. M. Truskett and S. Garde, Hydrophobic hydration from small to large lengthscales: Understanding and manipulating the crossover, *Proc. Natl. Acad. Sci. U. S. A.*, 2005, **102**, 9475–9480.
12 D. Ben-Amotz, Water-mediated hydrophobic interactions, *Annu. Rev. Phys. Chem.*, 2016, **67**, 617–638.
13 R. Zangi and B. J. Berne, Temperature dependence of dimerization and dewetting of large-scale hydrophobes: A molecular dynamics study, *J. Phys. Chem. B*, 2008, **112**, 8634–8644.
14 C. Ma, C. Wang, C. Acevedo-Vélez, S. H. Gellman and N. L. Abbott, Modulation of hydrophobic interactions by proximally immobilized ions, *Nature*, 2015, **517**(7534), 347–350.
15 C. Wang, C. Ma, H. Yeon, X. Wang, S. H. Gellman and N. L. Abbott, Nonadditive interactions mediated by water at chemically heterogeneous surfaces: Nonionic polar groups and hydrophobic interactions, *J. Am. Chem. Soc.*, 2017, **139**, 18536–18544.
16 K. L. Johnson, K. Kendall and A. D. Roberts, Surface energy and contact of elastic solids, *Proc. R. Soc. London, Ser. A*, 1971, **324**, 301–313.
17 P. Stock, T. Utzig and M. Valtiner, Direct and quantitative AFM measurements of the concentration and temperature dependence of the hydrophobic force law at nanoscopic contacts, *J. Colloid Interface Sci.*, 2015, **446**, 244–251.
18 I. T. S. Li and G. C. Walker, Signature of hydrophobic hydration in a single polymer, *Proc. Natl. Acad. Sci. U. S. A.*, 2011, **108**, 16527–16532.
19 H. Yeon, C. Wang, R. C. Van Lehn and N. L. Abbott, Influence of order within nonpolar monolayers on hydrophobic interactions, *Langmuir*, 2017, **33**, 4628–4637.
20 H. Gojzewski, M. Kappl and A. Ptak, Effect of the chain length and temperature on the adhesive properties of alkanethiol self-assembled monolayers, *Langmuir*, 2017, **33**, 11862–11868.
21 G. W. Bennett, A laboratory experiment on the boiling-point curves of non-azeotropic binary mixtures, *J. Chem. Educ.*, 1929, **6**, 1544–1549.
22 M. D. Porter, T. B. Bright, D. L. Allara and C. E. D. Chidsey, Spontaneously organized molecular assemblies. 4. Structural characterization of n-alkyl thiol monolayers on gold by optical ellipsometry, infrared spectroscopy, and electrochemistry, *J. Am. Chem. Soc.*, 1987, **109**, 3559–3568.
23 J. Florián and A. Warshel, Calculations of hydration entropies of hydrophobic, polar, and ionic solutes in the framework of the Langevin dipoles solvation model, *J. Phys. Chem. B*, 1999, **103**, 10282–10288.
24 J. Florián and A. Warshel, Langevin dipoles model for ab initio calculations of chemical processes in solution: Parametrization and application to hydration free energies of neutral and ionic solutes and conformational analysis in aqueous solution, *J. Phys. Chem. B*, 1997, **101**, 5583–5595.
25 Y. Marcus, The guanidinium ion, *J. Chem. Thermodyn.*, 2012, **48**, 70–74.
26 Y. Marcus, *Ions in Solution and their Solvation*, Wiley, Hoboken, NJ, 1st edn, 2015.
27 H. Hesske and K. Gloe, Hydration behavior of alkyl amines and their corresponding protonated forms. 1. Ammonia and methylamine, *J. Phys. Chem. A*, 2007, **111**, 9848–9853.
28 H. Wincel, Hydration energies of deprotonated amino acids from gas phase equilibria measurements, *J. Am. Soc. Mass Spectrom.*, 2008, **19**, 1091–1097.
29 B. Gao, T. Wyttenbach and M. T. Bowers, Protonated arginine and protonated lysine: Hydration and its effect on the stability of salt-bridge structures, *J. Phys. Chem. B*, 2009, **113**, 9995–10000.
30 C. Houriez, M. Meot-Ner and M. Masella, Solvation of the guanidinium ion in pure aqueous environments: A theoretical study from an "Ab initio"-based polarizable force field, *J. Phys. Chem. B*, 2017, **121**, 11219–11228.

